

- where  $I_{\text{total}}$  is the whole-cell current and  $i$  is the single-channel current. The modal weighting coefficients ( $A_{\text{low}}$ ,  $A_{\text{med}}$ ,  $A_{\text{high}}$ ) are those plotted in Fig. 3A and allow for the proportion of blank sweeps ( $A_{\text{blank}}$ ). The unitary currents were set at  $i_{\text{low}} = 0.9$  pA and  $i_{\text{med}} = i_{\text{high}} = 0.7$  pA (13). We determined the wave form of open probability [ $P_o(t)$ ] for each mode by averaging idealized records for all sweeps falling within the appropriate modal category.
19. The contribution of the medium- $P_o$  mode was only slightly decreased here. In earlier recordings taken under different experimental conditions (5), most of the current in control patches was supported by medium- $P_o$  gating, and NE produced a shift away from medium- $P_o$  to low- $P_o$  gating. In either case, the modulation favored a less active mode.
  20. S. W. Jones, *Biophys. J.* **60**, 502 (1991).
  21. L. M. Boland and B. P. Bean, *J. Neurosci.* **13**, 516 (1993). Boland and Bean propose a quantitative model where a single N-type  $\text{Ca}^{2+}$  channel can accommodate between zero and four G protein subunits. This would be most consistent with our results if N-type channels displayed four active patterns of gating. Our analysis has separated high-, medium-, and low- $P_o$  gating, but an additional distinction might be made between low- $P_o$  and  $O_a$ -type gating (33).
  22. With NE, typical sojourns in the high- $P_o$  mode were considerably briefer than the onset time constants of neurotransmitter inhibition, which were  $\sim 2$  s (12, 23). Sojourns in the low- $P_o$  mode were relatively long-lasting, consistent with the slow time constant of recovery from neurotransmitter inhibition, estimated as  $\sim 18$  s in these cells (20, 21).
  23. S. R. Ikeda, *J. Physiol. (London)* **439**, 181 (1991).
  24. In whole-cell recordings (Fig. 4C), pipettes contained a solution with 100 mM CsCl, 10 mM EGTA, 5 mM  $\text{MgCl}_2$ , 2 mM Na adenosine triphosphate, 0.3 mM Na guanosine triphosphate, and 40 mM Hepes (pH 7.3 with CsOH) and had resistances of  $\sim 2$  megohms. Gigaohm seals and whole-cell configuration were obtained with a bathing solution that contained 120 mM NaCl, 2 mM KCl, 10 mM glucose, and 10 mM Hepes (pH 7.3 with NaOH). For  $\text{Ba}^{2+}$  current recordings, the bathing solution was changed to one that contained 110 mM  $\text{BaCl}_2$ , 10 mM glucose, 100 nM tetrodotoxin, and 10 mM Hepes (pH 7.3 with TEA-OH).
  25. Although it is clear that prepulse-induced sojourns in the high- $P_o$  mode occasionally occurred, more extensive recordings are needed to characterize the kinetics of reinhibition at the unitary level. Our data are limited because the cell-attached patches were often destroyed by the strong prepulses needed to remove the inhibition.
  26. Slow relief of inhibition during the test pulse was not seen in our experiments (Fig. 1, insets), which is consistent with its variable occurrence in earlier experiments (1–12) depending on the test potential and the type and concentration of neurotransmitter. Slow deinhibition might not be expected under the experimental conditions used for the unitary recordings. The high NE concentration was chosen for a near-maximal degree of inhibition but would be expected to increase the amount of activated G proteins and thereby minimize the time-dependent relief of inhibition (4, 9–11). We chose relatively weak test depolarizations to keep unitary current large and to reduce open probability in the low- $P_o$  mode so that this activity would be easily distinguished from other modes; however, this would also hamper relief of inhibition, because channel opening in the reluctant mode is needed to drive off the inhibitory G protein (4, 11).
  27. Y. Kurachi, H. Ito, T. Sugimoto, *Pluegers Arch.* **416**, 216 (1990).
  28. J. Monod, J. Wyman, J.-P. Changeux, *J. Mol. Biol.* **12**, 88 (1965).
  29. In model A, the transition rate from low  $\rightarrow$  (blank/ $O_a$ ) should increase with the amount of activated G protein.
  30. Here, transitions between the high- $P_o$  and the low- $P_o$  modes were the most relevant because blank sweeps may reflect either G protein-mediated inhibition or merely inactivation. Figure 1A exemplifies a total of 13 high  $\rightarrow$  low and 9 low  $\rightarrow$  high transitions out of a total of 888 sweeps in control patches.
  31. Some intermediary sojourns in the medium- $P_o$  mode might be brief enough to go undetected, but this is highly unlikely in four consecutive instances because the apparent lifetime of medium- $P_o$  mode gating was relatively long (two and a half sweeps in the patch in Fig. 1, A and B).
  32. P. Hess, J. B. Lansman, R. W. Tsien, *Nature* **311**, 538 (1984); T. N. Marks and S. W. Jones, *J. Gen. Physiol.* **99**, 367 (1992).
  33. D. T. Yue, S. Herzog, E. Marban, *Proc. Natl. Acad. Sci. U.S.A.* **87**, 753 (1990).
  34. J. A. Bevan, F. M. Tayo, R. A. Rowan, R. D. Bevan, *Fed. Proc.* **43**, 1365 (1984).
  35. We are grateful to D. Lipscombe for her participation in the early stages of this project. We thank R. W. Aldrich, D. D. Friel, W. A. Sather, R. H. Scheller, J. Yang, and J.-F. Zhang for their comments on the manuscript, K. Bley and P. Rivas for help in preliminary experiments, and R. W. Aldrich for suggesting the model in Fig. 5B. This work was supported by a National Research Service Award (A.H.D.), Public Health Service grants NS24607 and HL13156, and the Silvio Conte Center of the National Institute of Mental Health at Stanford University.

24 August 1992; accepted 1 December 1992

## Shutdown of Class Switch Recombination by Deletion of a Switch Region Control Element

Steffen Jung,\* Klaus Rajewsky, Andreas Radbruch

Upon activation, B lymphocytes can change the class of the antibody they express by immunoglobulin class switch recombination. Cytokines can direct this recombination to distinct classes by the specific activation of repetitive recombinogenic DNA sequences, the switch regions. Recombination to a particular switch region ( $s_{\gamma 1}$ ) was abolished in mice that were altered to lack sequences that are 5' to the  $s_{\gamma 1}$  region. This result directly implicates the functional importance of 5' switch region flanking sequences in the control of class switch recombination. Mutant mice exhibit a selective agammaglobulinemia and may be useful in the assessment of the biological importance of immunoglobulin G1.

Immunoglobulin class switch recombination permits a B cell to sequentially express antibodies that have identical specificities but that differ in class and thus effector function. This recombination, which moves the variable region exon of the immunoglobulin heavy (IgH) chain to associate with a different set of constant region exons, is mediated by switch (s) regions—that is, arrays of short tandem repeats located upstream of each constant region ( $C_H$ ) gene segment, except  $C_{\delta}$ . Once activated, class switch recombination is a regulated process, directed to the same switch region on the active and the allelically excluded, inactive allele of a given B cell (1). Class switching is directed by cytokines. For example, the addition of interleukin-4 (IL-4) to cultures of polyclonally activated B cells induces switching to IgG1 and IgE (2). The direction of class switching may be determined by the modulation of accessibility of the individual switch regions to a common switch recombinase (3). Before recombination, 5' switch region flanking sequences are subjected to cytokine-induced demethylation (4) and chromatin changes (5). Furthermore, the activation of promoter and enhancer elements in these regions leads to transcription

of the respective unrearranged (germline) switch regions and their associated  $C_H$  genes (6). Despite the large body of correlative evidence for germline transcription and class switch recombination (3, 6), a functional relation between switch region flanking sequences and class switch recombination has not been directly shown.

To test the functional importance of switch region flanking sequences for switch recombination, we generated mutant mice that lack 5' flanking sequences of the  $s_{\gamma 1}$  switch region (7) (Fig. 1). The homologous recombination event yields an IgH locus with the 5'  $s_{\gamma 1}$  region being replaced by an inversely oriented neomycin resistance ( $neo^r$ ) gene needed for selection of recombinants in the conventional targeting scheme (8). In the targeting construct (9), the  $neo^r$ -cassette replaces 1.7 kb of the 5'  $s_{\gamma 1}$  region spanning all sites of molecular changes known to be induced by the cytokine IL-4—that is, a protein binding site (10), deoxyribonuclease (DNase) I hypersensitive sites (5), sites of specific demethylation (4), and the promoter elements and splice donor site of the  $I_{\gamma 1}$ -germline transcript (11) (Fig. 1D).

Using a murine embryonic stem (ES) cell line derived from 129/Ola mice ( $IgH^a$ ), we generated ES cell clones that were heterozygous for the targeted replacement of the 5'  $s_{\gamma 1}$  region (designated  $neo\Delta 5's_{\gamma 1}$ ) by homologous recombination (12). To exclude the influence of the  $neo^r$  gene or its control

Institute for Genetics, University of Cologne, D-5000 Cologne 41, Germany.

\*To whom correspondence should be addressed.

elements on class switch recombination, we subsequently deleted the *neo<sup>r</sup>*-cassette using the yeast Flp recombination system (13, 14). In the targeting construct (9), the *neo<sup>r</sup>* gene is flanked by two Flp recombination target (FRT) sequences oriented in parallel (Fig. 1). For site-specific deletion, we transiently transfected a targeted ES cell clone (clone 12) with the Flp recombinase expression vector pOG44 (14) and isolated an ES cell clone (clone 12.21) that had the desired deletion, designated  $\Delta 5's_{\gamma 1}$  (15). The resulting locus retains a single copy of an FRT signal. The structure of the targeted loci was confirmed by restriction analysis (Fig. 2).

Cells of three independent *neo* $\Delta 5's_{\gamma 1}$  ES cell clones (clones 13, 10, and 2) and the  $\Delta 5's_{\gamma 1}$  clone (clone 12.21) were injected into blastocysts of C57BL/6 and CB.20 mice to generate chimeric mice. The *IgH* allotype differences of ES cell (*IgH<sup>a</sup>*)-derived and blastocyst (*IgH<sup>b</sup>*)-derived cells allowed the analysis of B cells that were heterozygous (*IgH<sup>neo</sup> $\Delta 5's_{\gamma 1a/b}$*  or *IgH <sup>$\Delta 5's_{\gamma 1a/b}$</sup>* ) for the mutation in the chimeric mice; host-derived B cells are *IgH<sup>b/b</sup>*. To determine the effect of the deletion on IgG1 class switch recombination, we polyclonally activated splenic B cells from *neo* $\Delta 5's_{\gamma 1}$  and  $\Delta 5's_{\gamma 1}$  chimeras by bacterial lipopolysaccharide (LPS) in the presence of IL-4 (Table 1). After this treatment, B cells that carried a mutant allele showed a 50% reduction in the frequency of IgG1-expressing cells as compared to wild-type controls. Assuming equal representation of cells that expressed the mutant and the wild-type allele, cells that expressed the targeted allele probably had not switched to  $\gamma 1$ .

If this interpretation is correct, IgG1<sup>a</sup>-expressing B cells from *neo* $\Delta 5's_{\gamma 1}$  and  $\Delta 5's_{\gamma 1}$  chimeras should have functionally rearranged and switched the wild-type allele but left the targeted allele in germline configuration. A DNA restriction enzyme analysis of sorted cells that express  $\mu^a$  and  $\gamma 1^a$  from the culture (LPS plus IL-4) of *neo* $\Delta 5's_{\gamma 1}$  and  $\Delta 5's_{\gamma 1}$  chimeras confirmed this prediction (Fig. 3). The  $\gamma 1^a$ -expressing cells retained the mutated allele in germline configuration, whereas all wild-type alleles were rearranged. Thus, the mutations in the 5' flanking regions shut down switch recombination to  $s_{\gamma 1}$ . Splenic B cell cultures of both the *neo* $\Delta 5's_{\gamma 1}$  and the  $\Delta 5's_{\gamma 1}$  chimeric mice yielded the same results (Table 1 and Fig. 3), which demonstrates that the silencing of  $s_{\gamma 1}$  is not a result of the insertion of the *neo<sup>r</sup>* gene or its control elements.

Because germline transmission of the *neo* $\Delta 5's_{\gamma 1}$  mutation was obtained before transmission of the  $\Delta 5's_{\gamma 1}$  mutation and because both mutations show the same phenotype, further analyses were done on mice with the *neo* $\Delta 5's_{\gamma 1}$  mutation. After the mating of *neo* $\Delta 5's_{\gamma 1}$  chimeras to C57BL/6

and CB.20 mice, the offspring that were derived from chimeras with mutated ES cells were identified by coat color and tested by restriction analysis of tail DNA for transmission of the mutated allele (Fig. 2). In het-

erozygous mutant mice (*IgH<sup>neo</sup> $\Delta 5's_{\gamma 1a/b}$* ), targeted and wild-type alleles can be distinguished serologically by means of their allotype differences. Thus, we can quantitate the extent to which the  $s_{\gamma 1}$  region is silenced

**Fig. 1.** Strategy for deletion of the 5'  $s_{\gamma 1}$  flanking region. (A) Genomic structure of the murine  $s_{\gamma 1}$  wild-type locus (*IgH<sup>a</sup>*) and its 5' flanking sequence. Tandemly repeated 49-bp units are indicated as black bars; direct repeats are shown as striped boxes. A, Acc I; E, Eco RI; B, Bgl II; H, Hind III; X, Xmn I; Xb, Xba I; and S, Sca I. (B) The targeting vector, which contains the 9.7-kb Hind III–Sca I fragment from the 5'  $s_{\gamma 1}$  locus (9). (C) Structure of the resultant loci that either contain (*neo* $\Delta 5's_{\gamma 1}$ ) or do not contain ( $\Delta 5's_{\gamma 1}$ ) the *neo<sup>r</sup>* gene. Triangles indicate the primers used in the PCR screening for homologous recombinants (pair A and B) (12) and for detection of clones with *neo<sup>r</sup>* gene deletion (pair C and B) (15). Primer A: 5'-CCTGCGTGAATC-CATCTTG-3'; primer B: 5'-CCTTCATTCTAACCTGCC-3'; primer C: 5'-AACAGTCAGCACCTCA-CTC-3'. (D) Detail of targeted replacement of the 5'  $s_{\gamma 1}$  region (7) and site-specific *neo<sup>r</sup>* gene deletion. The FRT-*neo*-FRT cassette (1.4 kb) replaced a fragment of 1.7 kb that carried all the known sites of IL-4-induced molecular changes. M, site of demethylation (4); circle, protein binding sites (10); striped boxes, DNase I hypersensitive sites (5); promoter elements and the splice donor site of the *I<sub>\gamma 1</sub>*-germline transcripts (11) are shown schematically.

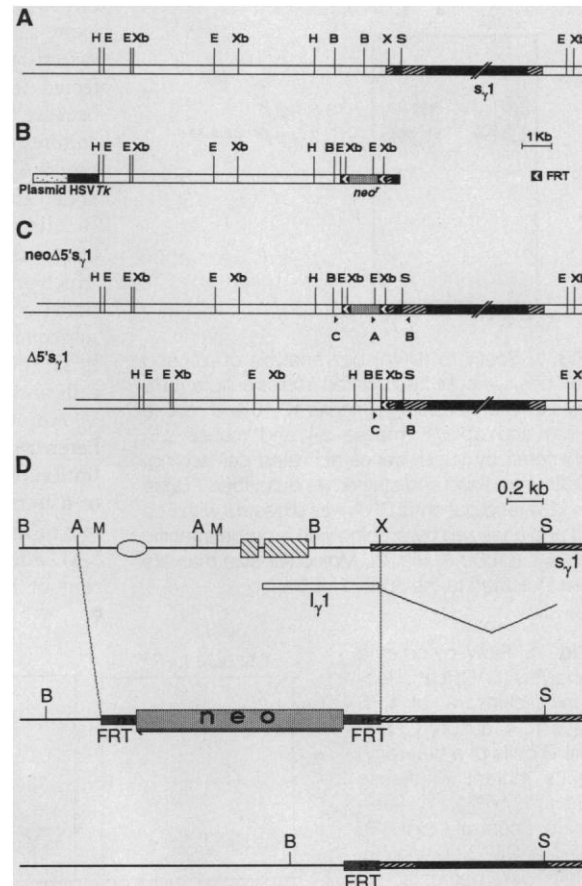
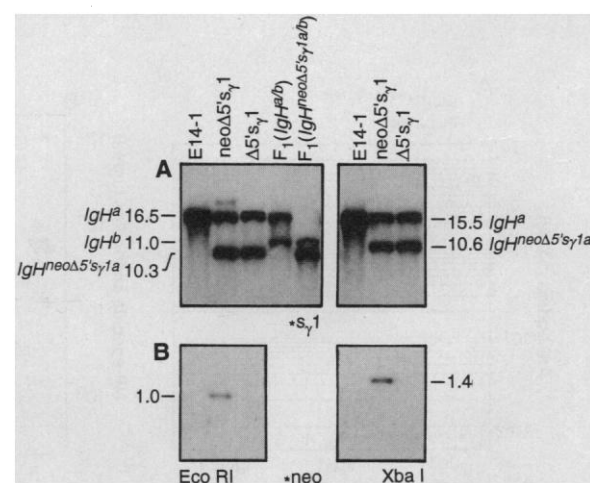


**Fig. 2.** Restriction analysis of wild-type E14-1, *neo* $\Delta 5's_{\gamma 1}$ , and  $\Delta 5's_{\gamma 1}$  cells and of F<sub>1</sub> heterozygous-mutant and wild-type ES cell-derived progeny of a *neo* $\Delta 5's_{\gamma 1}$  chimera resulting from matings with C57BL/6 mice. Genomic DNA was digested by Eco RI and Xba I. After gel electrophoresis and blotting, the upper half of the filter (A) was hybridized to probe A ( $s_{\gamma 1}$ ) (7) and the lower half (B) was hybridized to probe B (*neo*) (9). (A) The targeted ES cells (lanes 2, 3, 7, and 8) show the disruption of the 16.5-kb Eco RI and the 15.5-kb Xba I fragment of one of the wild-type *IgH<sup>a</sup>* alleles. Note that the  $\Delta 5's_{\gamma 1}$  cells retain the Xba I site indicative for the remaining FRT signal, as predicted for Flp-mediated recombination. Lane 4 reveals the Eco RI and Xba I restriction polymorphism of the wild-type *IgH<sup>a</sup>* and *IgH<sup>b</sup>* alleles, and lane 5 shows the disrupted *IgH<sup>a</sup>* allele (10.3 and 10.6 kb) in a heterozygous mutant mouse (*IgH<sup>neo</sup> $\Delta 5's_{\gamma 1a/b}$* ). (B) The *neo<sup>r</sup>*-specific probe B verifies the deletion of the *neo<sup>r</sup>* gene in the  $\Delta 5's_{\gamma 1}$  ES cell clone. Lanes 1 and 6, wild-type ES cells; lanes 2 and 7, *neo* $\Delta 5's_{\gamma 1}$ -targeted cells; lanes 3 and 8,  $\Delta 5's_{\gamma 1}$ -targeted cells; lane 4, wild-type [129/Ola (*IgH<sup>a/b</sup>*) × C57BL/6(*IgH<sup>b/b</sup>*)] F<sub>1</sub>; lane 5, heterozygous *neo* $\Delta 5's_{\gamma 1}$  mutant F<sub>1</sub> (*IgH<sup>neo</sup> $\Delta 5's_{\gamma 1a/b}$* ). Molecular size markers are indicated to the right and left in (A) and (B) in kilobases. Asterisks indicate probe used.



by the neo $\Delta 5's_{\gamma 1}$  mutation.

Splenic B cells of heterozygous mutants ( $IgH^{neo\Delta 5's_{\gamma 1a/b}}$ ) and wild-type littermate con-

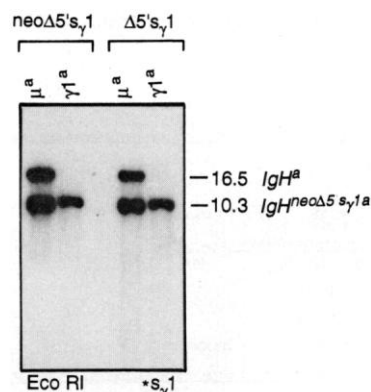


**Fig. 3.** Southern (DNA) blot analysis of  $\mu^a$ - and  $\gamma 1^a$ -positive cells fractionated from a culture (LPS plus IL-4) of neo $\Delta 5's_{\gamma 1}$  (mouse 10.10 and mouse 13.1) and  $\Delta 5's_{\gamma 1}$  (mouse  $\Delta 4$  and mouse  $\Delta 5$ ) chimeras by fluorescence-activated cell sorting. Cells were fixed and stained as described (Table 1) (25), and genomic DNA was digested with Eco RI and analyzed by probing with a probe specific for  $s_{\gamma 1}$  (probe A, Fig. 2). Molecular size markers are indicated to the right in kilobases.

**Fig. 4.** Flow cytometric analysis (FACSscan; Becton Dickinson) of LPS plus IL-4-cultured splenic B cells of a heterozygous mutant  $F_1$  mouse ( $IgH^{neo\Delta 5's_{\gamma 1a/b}}$ ), a littermate control ( $IgH^{a/b}$ ), and a C57BL/6 mouse. Cells were harvested after 6 days of culture, purified, and stained in the cytoplasm with fluorescein isothiocyanate-coupled goat antibodies to mouse IgG1, biotinylated mouse monoclonal antibody to mouse IgG1<sup>a</sup>, and streptavidin phycoerythrin (25). Dots refer to cells in the lymphocyte gate as defined by light scatter.

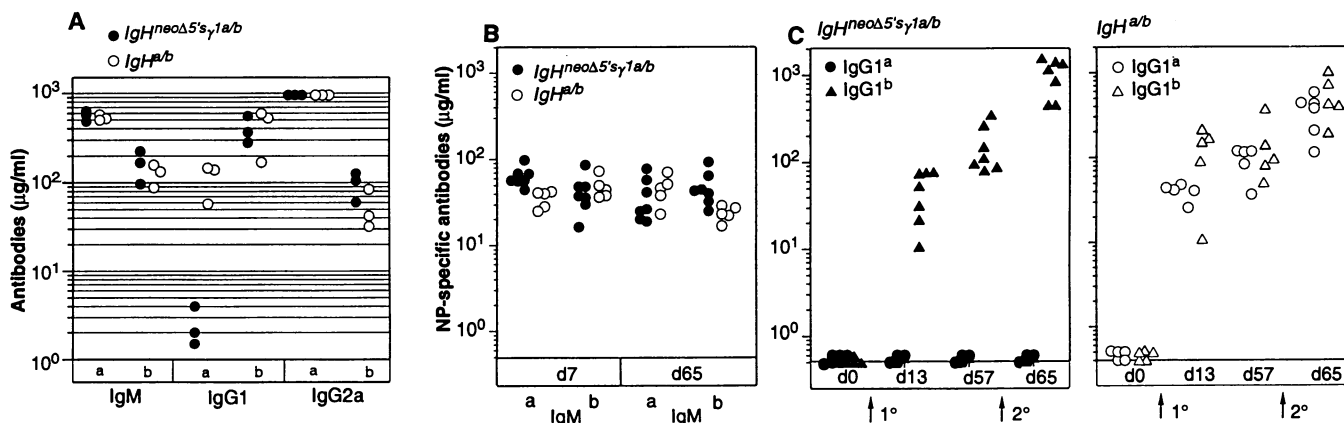
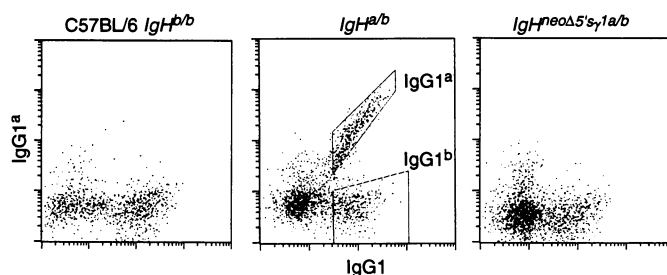


**Fig. 5.** Serum concentrations of Ig isotypes of unimmunized and NP-CG-immunized heterozygous mutant  $F_1$  mice and their wild-type littermate controls. (A) Six-week-old heterozygous mutant (●) and wild-type littermate control (○) animals were bled from the subcaudal vein, and serum titers of the indicated antibodies classes were determined by enzyme-linked immunosorbent assay as described (16). (B and C) Seven-week-old mice of both groups were immunized by intraperitoneal injection of

controls ( $IgH^{a/b}$ ) were activated in vitro with LPS or LPS plus IL-4 (Fig. 4 and Table 1). B cells of both allotypes from littermate control mice differentiated into IgG1-expressing cells; however, in heterozygous mutant mice B cells that expressed the targeted allele ( $IgH^{neo\Delta 5's_{\gamma 1a}}$ ) did not switch to IgG1. The frequency of IgG1<sup>a</sup>-expressing cells was reduced by 99.5%. Class switch recombination in general was not affected in the heterozygous mutant B cells because the frequencies of IgG3 cells in LPS cultures of wild-type and mutant mice were similar (Table 1). In cultures (LPS plus IL-4) of neo $\Delta 5's_{\gamma 1}$  and  $\Delta 5's_{\gamma 1}$  heterozygous mutant B cells, IgM-expressing cells appeared more frequently than in control cultures (Table 1), which suggests that these cells, which functionally rearranged the targeted allele but subsequently failed to switch to expression of IgG1, remained in the pool of IgM-expressing cells and did not switch to other classes.

An evaluation of serum antibody titers of heterozygous mutant mice revealed a concentration of IgG1<sup>a</sup> (2.5  $\mu$ g/ml) that was 2% that of littermate controls, whereas the serum titers of IgM and IgG2a were unchanged (Fig. 5A). After primary and secondary immunization of heterozygous mutant and littermate

control mice with (4-hydroxy-3-nitrophenyl)acetyl (NP)-chicken  $\gamma$ -globulin (CG) NP-specific antibody, titers were determined. The overall extent of the immune response was similar for both groups of mice, as reflected by the NP-specific IgM (Fig. 5B) and IgG1<sup>b</sup> (Fig. 5C) titers, but the concentration of NP-binding IgG1<sup>a</sup> (IgG1 derived from the  $IgH^{neo\Delta 5's_{\gamma 1a}}$  locus) in sera of heterozygous mutant mice was below our level of detection (60 ng/ml) (Fig. 5C). Thus, deletion of the 5'  $s_{\gamma 1}$  sequences affected IgG1 class switches in vitro and in vivo, which suggests the involvement of the 5'  $s_{\gamma 1}$  region in the control of both the IL-4-induced and the recently postulated IL-4-independent (16, 17) class switch to IgG1.

Our results show that a repetitive switch region devoid of its 5' flanking sequences is severely impaired as an acceptor for the common donor  $s_{\mu}$  region. These data establish the existence of spatially separated switch recombination substrate and recombination control elements. A similar bipartite structure with the IgH intron enhancer functioning as a recombinatorial enhancer has been suggested for the V(D)J joining (18). Stimulating recombination in adjoining sequences, the switch recombination control element is reminiscent of hot spots of recombination in yeast that promote homologous recombination of flanking DNA (19, 20).

The neo $\Delta 5's_{\gamma 1}$  allele remained inert even in cells heterozygous for the mutation ( $IgH^{neo\Delta 5's_{\gamma 1a/b}}$ ) with all potential transacting factors present (including the  $I_{\gamma 1}$  germline transcripts), as demonstrated by the ability of the wild-type allele to undergo class switching to IgG1. The cis-acting nature of the 5' switch region flanking elements is consistent with the current model that attributes directed class switch recombination

100  $\mu$ g of alum-precipitated NP-CG. Sera were taken on day 7 (d7; for IgM<sup>a</sup> and IgM<sup>b</sup> titers) and day 13 (d13; for IgG1 titers) after primary immunization (1°) and on day 7 after boosting (2°). Preimmune sera contained NP-binding IgM (2  $\mu$ g/ml) and NP-binding IgG1 (less than 60 ng/ml of either allotype). Responses of individual neo $\Delta 5's_{\gamma 1}$  heterozygous mutant mice (●) and wild-type littermate controls (○) are given.

**Table 1.** In vitro LPS culture analysis of splenic B cells from chimeric and heterozygous mutant mice. In the analysis of chimeras, the *IgH<sup>a</sup>* allotype represents the ES cell–derived B cells, whereas in the analysis of the heterozygotes it distinguishes cells that express the mutant *IgH* locus from the ones that express the wild-type *IgH* locus. The degree of chimerism in the B cell compartment varied from 75 to 100% ES cell–derived B cells in the individual chimeras. As a control for the chimera analysis, we used mice generated with ES cells that carried wild-type *IgH* loci. Data were evaluated with a FACScan (Becton Dickinson) (Fig. 4) and are listed as percent positive cells per B cell blasts and percent of  $\kappa$  and  $\lambda$  positive cells, respectively. Dashes indicate data not determined.

Mouse	IgH genotype	LPS			LPS + IL-4			
		$\gamma$ 3	$\mu$	$\gamma$ 1	$\gamma$ 1 <sup>a</sup>	$\mu$ <sup>a</sup>	$\gamma$ 1 <sup>b</sup>	$\mu$ <sup>b</sup>
<i>Chimeric mice</i>								
1	<i>a/a</i>	—	—	—	25	22	—	—
2	<i>a/a</i>	—	—	—	26	20	—	—
3	<i>a/a</i>	—	—	—	20	37	—	—
13.1	<i>neoΔ5's<sub>γ</sub>1a/a</i>	—	—	—	10	30	—	—
10.10	<i>neoΔ5's<sub>γ</sub>1a/a</i>	—	—	—	10	32	—	—
10.4	<i>neoΔ5's<sub>γ</sub>1a/a</i>	—	—	—	13	36	—	—
2.4	<i>neoΔ5's<sub>γ</sub>1a/a</i>	—	—	—	12	38	—	—
Δ10	<i>Δ5's<sub>γ</sub>1a/a</i>	—	—	—	13	22	—	—
Δ11	<i>Δ5's<sub>γ</sub>1a/a</i>	—	—	—	13	17	—	—
Δ4	<i>Δ5's<sub>γ</sub>1a/a</i>	—	—	—	14	28	—	—
Δ5	<i>Δ5's<sub>γ</sub>1a/a</i>	—	—	—	13	35	—	—
<i>Heterozygous mutant mice</i>								
1	<i>a/b</i>	16	16	—	20	4	17	13
2	<i>a/b</i>	19	13	—	22	5	18	9
3	<i>neoΔ5's<sub>γ</sub>1a/b</i>	19	16	0.9	0.3*	14	23	10
4	<i>neoΔ5's<sub>γ</sub>1a/b</i>	16	15	1.2	0.1†	11	25	15
Control	<i>b/b</i>	10	18	—	0.1	0.1	42	—

\*This value has been confirmed by fluorescence microscopy to be 0.08% of  $\kappa$  and  $\lambda$  positive cells. †This value has been confirmed by fluorescence microscopy to be 0.15% of  $\kappa$  and  $\lambda$  cells.

to modulation of the accessibility of the individual switch regions (3). Yet, it remains unknown how the control region exerts its influence on the switch region. Despite the correlation of cytokine-induced, class-specific transcription of switch regions and the direction of recombination (6) and recent experiments that show that transcriptional regulatory elements increase the frequency of recombination on extrachromosomal switch recombination substrates (21), the causal relation of germline transcription and class switch recombination is still unclear. Thus, the 1.5-kb 5's<sub>γ</sub>1 fragment we deleted may well carry an inducible recombination enhancing element overlapping with, but distinct from, the I<sub>γ</sub>1 promoter, as recently reported for the recombination initiation site and the promoter of ARG4 in yeast (22).

Future studies with mice that lack the 5' s<sub>γ</sub>1 flanking sequences will reveal the role of sequential switch recombination via IgG1, recently proposed to impose an additional control on the expression of IgE (23). Exhibiting a selective IgG1 immune deficiency, Δ5's<sub>γ</sub>1 homozygous mutant mice will allow studies of the importance of class switching to IgG1 in the humoral immune response and for the establishment of immunologic memory.

REFERENCES AND NOTES

1. A. Radbruch, W. Müller, K. Rajewsky, *Proc. Natl. Acad. Sci. U.S.A.* **83**, 3954 (1986).  
 2. P. C. Isakson *et al.*, *J. Exp. Med.* **155**, 734 (1982); S.

Bergstedt-Lindqvist *et al.*, *Eur. J. Immunol.* **18**, 1073 (1988); C. Esser and A. Radbruch, *Annu. Rev. Immunol.* **8**, 717 (1990).  
 3. G. Yancopoulos *et al.*, *EMBO J.* **5**, 3259 (1986); J. Stavnezer-Nordgren and S. Sirlin, *ibid.*, p. 95.  
 4. C. Burger and A. Radbruch, *Eur. J. Immunol.* **20**, 2285 (1990).  
 5. J. Schmitz and A. Radbruch, *Int. Immunol.* **1**, 570 (1989).  
 6. C. Esser and A. Radbruch, *EMBO J.* **8**, 483 (1989); D. Leberman *et al.*, *J. Immunol.* **144**, 952 (1990); P. Rothman *et al.*, *J. Exp. Med.* **168**, 2385 (1988); P. Rothman *et al.*, *Int. Immunol.* **2**, 621 (1990); E. Severinson *et al.*, *Eur. J. Immunol.* **20**, 1079 (1990); M. Berton, *et al.*, *Proc. Natl. Acad. Sci. U.S.A.* **86**, 2829 (1989).  
 7. M. Mowatt and W. Dunnick, *J. Immunol.* **136**, 2674 (1986) [s<sub>γ</sub>1 sequence; GenBank M12389]. Because the 3' end of the deleted I<sub>γ</sub>1 pseudoexon coincides with the most 5' element of the switch region (Fig. 1D), our deletion led to the removal of 96 bp of the 330 bp that span direct repeat II. The direct repeats I and II are a unique feature of the s<sub>γ</sub>1 switch region, and all the known recombination breakpoints of s<sub>μ</sub>-s<sub>γ</sub>1 hybrids fall within the repetitive region. Thus, we tend to define the recombinogenic switch region by the latter.  
 8. S. L. Mansour *et al.*, *Nature* **336**, 348 (1988).  
 9. For construction of the targeting vector, a *neo<sup>r</sup>* gene {modified from pMC1neo-poly(A) [K. R. Thomas and M. R. Cappecci, *Cell* **51**, 503 (1987)]} was flanked by two FRT signals isolated as Hind II–Eco RI fragments from plasmid pOG45 [(14); Stratagene]. The resulting Xho I–Sal I FRT–*neo<sup>r</sup>*–FRT cassette (1.4 kb) was inserted between an Acc I site [position 310 (7)] and an Xmn I site (position 2014) in a plasmid that carried the 5' s<sub>γ</sub>1 region subcloned from plasmid pγ1/EH10.0 (7). The fragment was inserted into pIC19R/MC1-TK (8), and the 5' homologous region was elongated by insertion of an 8-kb Hind III fragment isolated from Charon γ1-13 [A. Shimizu, N. Takahashi, Y. Yaoita, T. Honjo, *ibid.* **28**, 499 (1982)]. Before transfection, the final vector (Fig. 1B) was linearized at a newly generated Not I site, which replaced the Sca I site (position 2881).

10. H. Illges and A. Radbruch, *Mol. Immunol.* **29**, 1265 (1992).  
 11. M. Xu and J. Stavnezer, *Dev. Immunol.* **1**, 11 (1990); *EMBO J.* **11**, 145 (1992).  
 12. E14-1 cells, a subclone of the ES cell line E14 [M. Hooper, K. Hardy, A. Handyside, S. Hunter, M. Monk, *Nature* **326**, 292 (1987)] were cultured in Dulbecco's modified Eagle's medium supplemented with 15% fetal calf serum, 0.1 mM β-mercaptoethanol, 1 mM sodium pyruvate, and a saturating amount of myeloid leukemia inhibitory factor [R. L. Williams *et al.*, *ibid.* **336**, 685 (1988)] on mitomycin C–treated primary embryonic fibroblasts prepared from embryos transgenic for a *neo<sup>r</sup>* gene. The cells were electroporated with the linearized targeting vector (20 μg/ml), subjected to double selection with G418 (250 μg/ml) and Ganciclovir (2 μM) (8), and screened for homologous recombination by polymerase chain reaction (PCR) (24) with the primer pair A and B (Fig. 1C). From 24 single colonies analyzed, nine were positive and further characterized (Fig. 2). Transfection of 5 × 10<sup>7</sup> cells yielded 9 × 10<sup>3</sup> G418-resistant colonies (as determined by control plates). Of these, 2.7 × 10<sup>3</sup> had stably integrated the *neo<sup>r</sup>* gene but not the *HSVtk* gene. The frequency of homologous recombinants was one-third of G418-Ganciclovir double-resistant colonies.  
 13. J. R. Broach and J. B. Hicks, *Cell* **21**, 501 (1980).  
 14. S. O'Gorman, D. T. Fox, G. M. Wahl, *Science* **251**, 1351 (1991).  
 15. The Flp recombinase–mediated deletion of the *neo<sup>r</sup>* gene was achieved by transient transfection of a *neoΔ5's<sub>γ</sub>1* targeted ES cell clone with the Flp recombinase expression vector pOG44 [(14); Stratagene]. Two days after transfection with the Bio-Rad gene pulser (with a transient transfection efficiency of approximately 5% as determined by lacZ control transfections), the cells were replated at low density (1 × 10<sup>3</sup> cells per 10-cm dish). Pooled samples of six colonies were analyzed on day 15 by PCR with the primer pair C and B. One out of 192 colonies tested was positive for the deletion, as verified by restriction analysis (Fig. 2).  
 16. R. Kühn, K. Rajewsky, W. Müller, *Science* **254**, 707 (1991).  
 17. C. Schultz *et al.*, *J. Immunol.* **149**, 60 (1992).  
 18. P. Ferrier *et al.*, *EMBO J.* **9**, 117 (1990).  
 19. A. Nicolas *et al.*, *Nature* **338**, 35 (1989).  
 20. K. Voelkel-Meiman *et al.*, *Cell* **48**, 1071 (1987).  
 21. H. Leung and N. Maizels, *Proc. Natl. Acad. Sci. U.S.A.* **89**, 4154 (1992).  
 22. N. Schultes and J. Szostak, *Mol. Cell. Biol.* **11**, 322 (1991).  
 23. G. Siebenkotten *et al.*, *Eur. J. Immunol.* **22**, 1827 (1992); F. Mills *et al.*, *J. Immunol.* **149**, 1075 (1992).  
 24. D. Kitamura *et al.*, *Nature* **350**, 423 (1991).  
 25. LPS cultures were carried out as described (23). On day 6 of culture, cells were harvested, purified on a Ficoll gradient, and fixed in 70% methanol before cytoplasmic staining. Fluorescent conjugates of the following antisera and monoclonal antibodies were used: goat–anti-mouse IgG3 [Southern Biotechnology Associates, Birmingham, Alabama (SBA)], goat–anti-mouse IgG1 (SBA), R33-24-12 (anti-μ), RS3.1 (anti-μ<sup>a</sup>), MB86 (anti-μ<sup>b</sup>), and 20.9 Ig4(a) (anti-IgG1<sup>a</sup>) (16, 24). IgG1<sup>b</sup>-positive cells were determined as being IgG1<sup>+</sup> and IgG1<sup>a-</sup>. For IgG3-positive cells, no allotype distinction was possible.  
 26. We thank H. Illges, J. Irsch, J. Schmitz, G. Siebenkotten, W. Mueller, R. Dilldrop, B. Kemper, and the Cologne ES cell group for discussions and advice; Genetics Institute for an LIF-producing cell line; A. Tarakhovskiy for control chimeras; S. Irlenbusch, C. Uthoff-Hachenberg, and C. Goettlinger for technical help; and U. Ringeisen for preparation of figures. Supported by the Bundesministerium für Forschung und Technologie through Genzentrum Köln, by Deutsche Forschungsgemeinschaft, the Fazit Foundation, and the Human Frontier Science Program Organization.

2 October 1992; accepted 9 December 1992